Supporting Information

Paquay et al. 10.1073/pnas.0908874106

SI Text

Exposures of the YD black mats with reliable ^{14}C dates were sampled and analyzed for PGE content and Os isotopic composition. For example, the Gainey Site that showed high concentrations of magnetic spherules and therefore high Ir concentration was not studied here because the age model from this section is poorly defined. Allen West provided samples of the black mat layer from Howard Bay, NC (level HB-11D2) and Blackwater Draw (NM) (levels BW-DT, D/C and BW-B/A) (1), similar to those measured in Firestone et al. (2). The Lommel, Maatheide section (Belgium), where the Usselo paleosoil horizon is well defined, yielded by far the highest Ir concentration [117 ng/g in the separated magnetic fraction (2)]. The sand and black mat layer at this site was resampled in detail.

The Lubbock Lake (TX), Topper section (SC) and a set of samples from Murray Springs from different trenches and profiles (Trench 22-Profile B1–B3) were also analyzed. Dolores Hill provided the Murray Springs samples that are splits of those used in the Firestone et al. study (2). The age model for these samples is constrained by multiple ^{14}C dates (3). These sediments are mostly fine to coarse, fluvial to lacustrine sands, clays or muds with an organic rich black mat layer.

Two sets of samples from glacial Lake Hind (Flintstone Hill section, Manitoba, Canada) were also sampled on two separate occasions. Each set is from the same location and no lithological differences were observed between the two sets of samples. One of the sample sets yielded several elevated iridium concentrations (≈4 ng/g) (2, 4) distributed over a ≈6-cm interval with a background level of ≈1 ng/g Ir. Such high background values are clear example of the analytical issues from (2), knowing that Ir concentration is (22 pg/g) for the average upper continental crust (5). The BA/YD transition at Lake Hind is derived by the linear extrapolation of the sedimentation rate from an AMS radiocarbon date of 10,420 ± 70 years BP (12,677–11,991 cal BP (6). Additionally, this age estimate is supported by a radiocarbon date of 12.76 ka BP from the base of the peat, as reported in Firestone et al. (2). The BA/YD is thought to occur within the lithologic change from massive carbonate-rich clay to silty clay onto a peat with alternating silty clay and organic laminae, coinciding with a decrease in water level (6).

The two marine sediments records, DSDP 480 (Deep Sea Drilling Project) (Gulf of California, (27°54.10′N, 111°39.34′W) and ODP (Ocean Drilling Program) 1002C (Cariaco Basin, 10°40′N, 65°00′W) (Fig. S1) have high organic carbon content and high accumulation rate (7, 8) ideal to reconstruct the seawater Os isotopic composition at high resolution (9). The age control of the YD interval in DSDP Site 480-core 3H is well constrained by ^{14}C dates [with a reservoir correction of 750 years (10)] on planktonic foraminifera at the onset, during and at the end of the YD (7, 11). At this site, the BA/YD transition shows a change in the oxygenation of the seafloor from laminated, biogenic silica-rich and carbonate-poor (2% $CaCO_3$) to non-laminated and more carbonate-rich sediments (≈13% $CaCO_3$). The YD/Holocene transition is marked by an abrupt return to laminated sediments. Sediments are organic-rich (2.2–4.9% TOC). The sedimentation accumulation rate throughout the YD averages 75 cm ka.

ODP Site 1002C sediments consist of anoxic and laminated organic-rich silts during the YD interval (4–5% TOC). The age model is derived from a correlation to the GISP2 core time scale (12). The sedimentation rate through the interval studied averages 35 cm ka. Each bulk sample (20 cm^3) represents an integrated time of ≈20 years for Site 480 and ≈60 years for Site 1002C.

Each sample was oven-dried at 60 °C for several days until constant sample weight was obtained. Samples were carefully isolated to avoid any contamination between potentially high- and low-iridium concentration samples. Sediments were disaggregated with a mortar and pestle. Homogenized powders were stored in a plastic beaker and isolated until further analysis. The determination of Os isotope ratios and Pt, Ir, and Os concentrations was carried out at the University of Hawaii. The same sediment powder was analyzed for all of the PGEs (Ir, Ru, Rh, Pt, Pd, Au) except Os at Ghent University.

Analytical Methodology for PGE (Ghent University). The PGEs (except for Os that volatilizes during the applied procedure) and Au concentrations were determined by using a nickel-sulfide fire-assay preconcentration method in combination with subsequent analysis using an ELAN DRC*plus* quadrupole-based ICP-MS instrument following the procedure described by Plessen and Erzinger (13) and Tagle and Claeys (14). A flux of 30 g of sodium carbonate, 60 g of sodium tetraborate, 5 g of calcium fluoride, 5 g of sulfur, and 5 g of nickel powder was added to the powdered samples, weighing between 13 and 70 g (pure SiO_2 powder was added when necessary). All reagents were of analytical grade and have been tested for PGE content. These mixtures were homogenized with an agate pestle, transferred into clay crucibles, and heated in a furnace at 1,150 °C for 1 h. After cooling, the nickel sulfide beads were separated from the slag by breaking the crucibles, subsequently ground, and dissolved in concentrated HCl in a hot water bath at 90 °C for 14 h. The residues were separated by filtration through glass micro filter devices (Schott, porosity 4), dissolved with a mixture of 2 parts of HCl (32 vol %, doubly distilled) and one part of H_2O_2 (30 vol %, analytical grade) in two subsequent steps, passed through a filter paper, and evaporated on a hotplate to a volume of 1–2 mL. After adding a final 5 mL of HCl and 2 mL of H_2O_2, the solution was evaporated to 1–2 mL, cooled, and diluted with 2 vol % HCl to a volume of 10 mL. Once In and Tl had been added as internal monitors, each solution was measured twice on separate measuring days for their ^{99}Ru, ^{101}Ru, ^{102}Ru, ^{103}Rh, ^{105}Pd, ^{106}Pd, ^{108}Pd, ^{191}Ir, ^{193}Ir, ^{194}Pt, ^{195}Pt, ^{196}Pt, and ^{197}Au concentrations by using external calibration solutions. Mathematical corrections were applied for isobaric interferences where necessary. The results obtained for international reference materials, a diabase TDB-1 with low PGE abundances and an altered peridotite WPR-1 with high PGE concentrations (Canadian Certified Reference Materials Project, CCRMP), are consistent with the certified data (15) and the recommended values of Meisel and Moser (16) (Table S1). These authors propose to compare new PGE data not only with the original certified values, but also with their compiled literature values until the certified values are up to date. Additionally, the precision and accuracy of the method are regularly tested by the analyses of a set of laboratory working standards (Popigai impact melt material, KT boundary clays, and meteorites). To determine the procedural detection limits (the instrumental detection limits are significantly lower), procedural PGE blank are determined by substituting the real samples with SiO_2 powder; omission of such a PGE-low substitute would result in a destruction of the clay crucibles by the aggressive fire assay flux. In this work, limit of detection (LOD) and limit of quantification (LOQ) are calculated as respectively 3 and 10 times the standard deviation (3 SD and 10 SD σ) on 10 reagent

blanks. The measured values below the LOD are reported as ND, not detected, whereas concentrations below the LOQ are indicated as <numeral value of the LOQ in Table S1.

Analytical Methodology for $^{187}Os/^{188}Os$ Ratio, Ir, Pt, and Os Concentrations (University of Hawaii). Os, Pt, and Ir were preconcentrated from bulk sediment samples by using a NiS fire assay. The amount of chemical fluxes was adjusted as a function of organic matter content. Each sample powder was accurately weighted (6–10 g) and spiked with a tracer solution enriched in ^{105}Pd, ^{190}Os, ^{191}Ir, and ^{198}Pt before fusion for concentration determination by isotope dilution. Isotope ratio measurements were made by using a magnetic-sector inductively coupled plasma mass spectrometer (ELEMENT2) according to a procedure slightly modified from that of Hassler et al. (17) where the OsO_4 becomes volatile after gassing into the vial by an argon stream into a torch and then transferred directly into the plasma.

An in-house standard is analyzed every five to six samples in each run to monitor the reproducibility. The average $^{187}Os/^{188}Os$ of these standards is 0.1082 ± 0.0028 (2 SD; n = 20). Ten procedural fusion blanks are carried out during the course of this study. The fusion blanks yielded an average of 0.64 ± 0.20 pg/g of reagents for Os and 1.5 ± 0.05 pg/g for Ir for a total weight of 31.5 g. Argon gas blanks are measured every set of five to six Os isotope analyses to monitor potential carryover of osmium between analyses. Iridium and platinum analyses are carried out on the same aliquot of powder split after $^{187}Os/^{188}Os$ analysis. Analytical uncertainties in Os concentration from the terrestrial sections are based on counting's statistics and are all ≤2%.

We estimate that the ^{187}Re in situ decay into ^{187}Os is unimportant because the sediments studied are recent. Therefore, no age correction was applied to the sediments.

1. Haynes CV, Jr (1995) Geochronology of Paleoenvironmental change, Clovis type Site, Blackwater Draw, New Mexico. *Geoarchaeology* 10:317–388.
2. Firestone RB, et al. (2007) Evidence for an extraterrestrial impact 12,900 years ago that contributed to the megafaunal extinctions and the Younger Dryas cooling. *Proc Natl Acad Sci USA* 104:16016–16021.
3. Jull AJ, Haynes CV, Donahue DJ, Burr GS, Beck JW (1998) Radiocarbon ages at Murray Springs, Arizona and the influence of climate change on Clovis Man. *Revue Archae* Suppl:339–343.
4. Kennett DG, et al. (2009) Nanodiamonds in the Younger Dryas boundary sediment layer. *Science* 323:94.
5. Peucker-Ehrenbrink B, Jahn B-M (2001) Rhenium–osmium isotope systematics and platinum-group element concentrations: Loess and the upper continental crust. *Geochem Geophys Geosyst* 2, 10.1029/2001GC000172.
6. Boyd M (2003) Paleoecology of an early Holocene wetland on the Canadian prairies. *Geogr Phys Quat* 57:139–149.
7. Barron JA, Bukry D, Bischoff JL (2004) High resolution paleoceanography of the Guaymas Basin, Gulf of California, during the past 15000 years. *Mar Micropaleontol* 50:185–207.
8. Peterson LC, et al. (2000) Late quaternary stratigraphy and sedimentation at Site 1002, Cariaco Basin (Venezuela). *Proceedings of the Ocean Drilling Program, Scientific Results*, eds Leckie RM, Sigurdsson H, Acton GD, Draper G (Ocean Drilling Program, College Station, TX), Vol 165, pp 85–99.
9. Paquay FS, Ravizza GE, Dalai TK, Peucker-Ehrenbrink B (2008) Determining chondritic impactor size from the marine osmium isotope. *Science* 320:214–218.
10. Keigwin LD (2002) Late Pleistocene–Holocene paleoceanography and ventilation of the Gulf of California. *J Oceanogr* 58:421–432.
11. Keigwin LD, Jones GA (1990) Deglacial climatic oscillation in the Gulf of California. *Paleoceanography* 6:1009–1023.
12. Hughen K, et al. (2004) 14C activity and global carbon cycle changes over the past 50,000 years. *Science* 303:202–207.
13. Plessen H-G, Erzinger J (1998) Determination of the platinum-group elements and gold in twenty rock reference material by inductively coupled plasma-mass spectrometry (ICPMS) after pre-concentration by nickel fire assay. *Geostandards Newslett* 22:187–194.
14. Tagle R, Claeys P (2005) An ordinary chondrite impactor for the Popigai crater, Siberia. *Geochim Cosmochim Acta* 69:2877–28889.
15. Govindaraju K (1994) Compilation of working values and description for 383 geostandards. *Geostandards Newslett* 18:1–154.
16. Meisel T, Moser J (2004) Reference materials for geochemical PGE analysis: New analytical data for Ru, Rh, Pd, Os, Ir, Pt and Re by isotope dilution ICP-MS in 11 geological reference materials. *Chem Geol* 208:319–338.
17. Hassler DR, Peucker-Ehrenbrink B, Ravizza GE (2000) Rapid determination of Os isotopic composition by sparging OsO_4 into a magnetic-sector ICP-MS. *Chem Geol* 166:1–14.
18. Kennett DG (2009) Shock-synthesized hexagonal diamonds in Younger Dryas boundary sediments. *Proc Natl Acad Sci USA* 106:12623–12628.
19. Wasson JT, Kallemeyn G (1989) Compositions of chondrites. *Phil Trans R Soc London Ser A* 325:105–127.

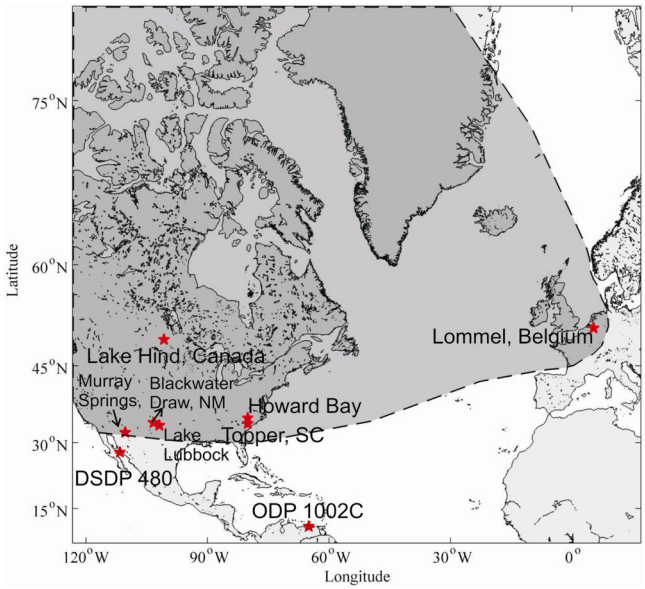

Fig. S1. Locations of the terrestrial and marine BA/YD sections analyzed in this study (red stars). The shaded area represents the approximated geographical extent of the nanodiamond fluence based on the report of nanodiamonds findings (4, 18).

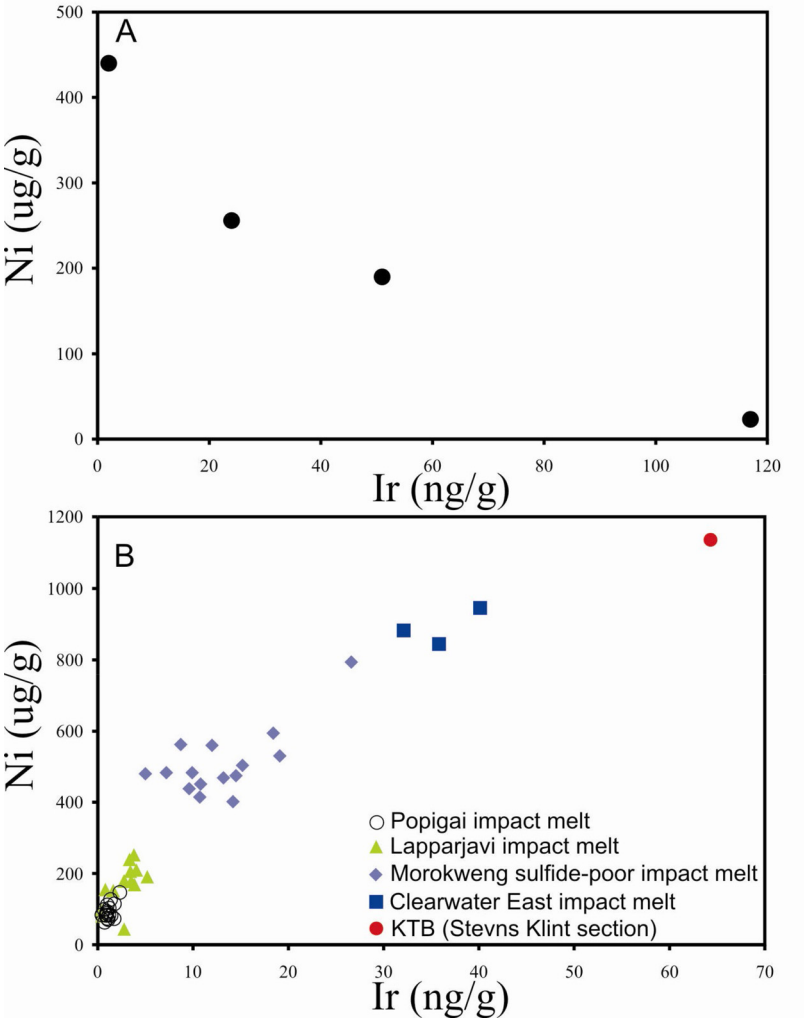

Fig. S2. (*A*) Ni-Ir concentrations in the black mat layer according to (2). (*B*) Positive Ni–Ir correlation in impact crater materials and KT ejecta layer. Note that the inverse Ni–Ir correlation in data from ref. 2 are uncharacteristic of impact products.

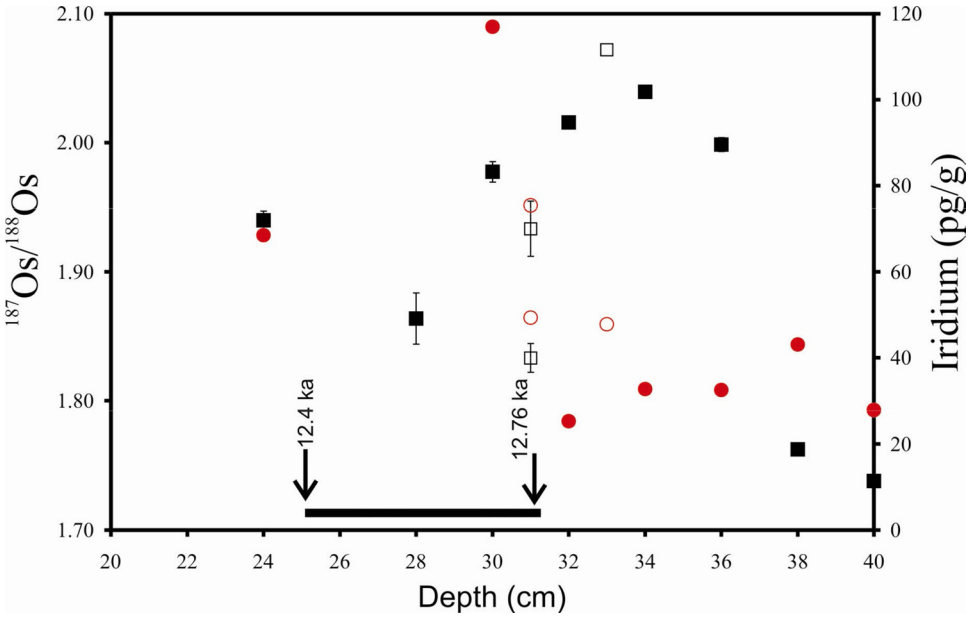

Fig. S3. $^{187}Os/^{188}Os$ ratios (open squares: batch 1 and filled squares: batch 2) and Ir concentrations (open circles: batch 1 and filled circles: batch 2) from the Lake Hind section. The 12.4-ka age is derived from ref. 6, whereas the 12.76-ka age datum is based on bulk ^{14}C (represented by arrows) reported in refs. 2 and 4. The depth scale (in centimeters) is derived from ref. 6. The horizontal bar represents the approximate depth interval where high Ir concentrations were previously reported (2).

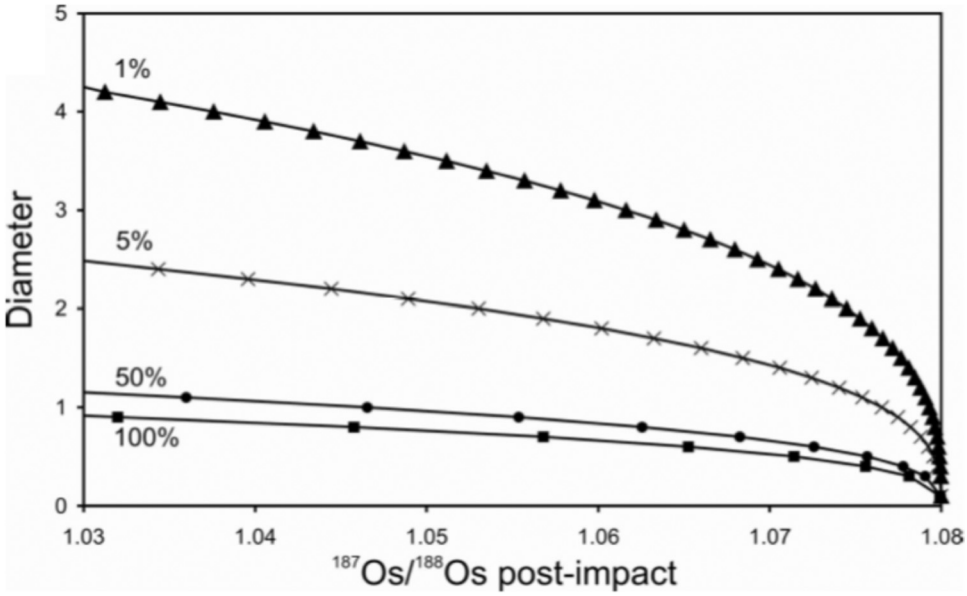

Fig. S4. Sensitivity of the marine $^{187}Os/^{188}Os$ record (Gulf of California dataset) to an alleged carbonaceous chondritic impactor ($^{187}Os/^{188}Os \approx 0.13$; averaged Os concentration of 650 ng/g (19) and density of 3.0 g cm^{-3} (http://meteorites.wustl.edu/id/density.htm), as a function of varying projectile diameters and varying fraction of Os vaporized (1–5-50–100% of projectile Os inventory) and soluble in seawater. These averaged concentrations and density values are based on the type of suggested projectiles (2). The calculations assume a global distribution of the extraterrestrial PGE fallout subsequently mixed to deep-sea sediments. Dissolution of projectile-derived Os over only a restricted region of the ocean would amplify the magnitude of the Os isotope excursion.

Table S1. $^{187}Os/^{188}Os$ ratios, and PGE's concentrations from the sections studied here (Howard Bay, Blackwater Draw, Murray Springs, Lubbock Lake, Topper, Lommel) compared with the averaged crustal material, the KT boundary at Fonte D'Olio (Italy) and the Clearwater East impact

Sample	$^{187}Os/^{188}Os$	2 SD	Os, pg/g	Ir (UH), pg/g	Pt (UH), pg/g	Ir VUB, pg/g	Ru VUB, pg/g	Rh VUB, pg/g	Pt VUB, pg/g	Pd VUB, pg/g	Au VUB, pg/g
Howard Bay 11D2	1.010	0.029	2	7	148	<42	200	38	<107	180	150
Howard Bay 11D2 REP	0.901	0.019	2	ND	ND	<42	<60	<36	<107	150	190
Blackwater Draw DT	1.343	0.004	435	41	1151		<60	44	400	1300	1120
Blackwater Draw DT REP	1.347	0.002	99	16	1874						
Blackwater Draw DC	1.343	0.003	298	11	194		<60	42	31	930	420
Blackwater Draw DC REP	1.334	0.003	80	10	446						
Blackwater Draw BW BA	1.353	0.007	45	47	388		<60	<36	390	160	<140
Blackwater Draw BW BA REP	1.385	0.004	7								
Lubbock Lake	ND		ND			<42	<60	<36	<107	290	564
Topper	ND		ND			46	239	<36	173	196	264
Lommel, Belgium	ND			20	47	<42	<60	<36	120	170	280
MS16MSO8/F2b2*	1.606	0.008	25								
MS16MSO8 REP/F2b2*	1.593	0.003	49	15	149						
MS26 MSO7/F2-F1a*	1.611	0.014	111	17	472	72	<60	<36	570	880	1600
MS5MSO8/F1a1*	1.378	0.009	100	49	435						
MS5MSO8 REP/F1a1*	1.365	0.005	90	31	320						
MS7aMSO8 REP/F2-D*	1.539	0.011	317	77	182						
MS6MSO8/F1*	1.677	0.039	6	25	74						
MS6MSO8 REP/F1*	1.648	0.017	6	19	58						
MS4MSO8/F2a1a*	1.652	0.011	88	25	429	48	<60	<36	400	860	2100
MS4MSO8 REP/F2a1a*	1.649	0.009	109	71	484						
Average continental crust†	1.260		31			22	210	60	510	520	2500
KT Fonte D'olio, Italy ($n = 3$)						6.93E+03	7.30E+03	1.74E+03	5.66E+03	6.24E+03	1.66E+03
Clearwater East impact melt‡			2.80E+04			2.90E+04	4.70E+04	1.40E+04	1.53E+05	1.24E+05	3.50E+04
CI (Tagle and Berlin, 2008)						4.72E+05	7.17E+05	1.35E+05	9.59E+05	5.63E+05	1.39E+05
LOD						13	18	11	32	40	42
LOQ						42	60	36	107	133	140

ND, not determined.

*Murray Springs section (AZ). The symbols associated to each sample stand for the following: from Murray Springs, Profile B1 (North of Area 1); From Murray Springs Profile B3 (3 m West of Profile B1), from bottom to top: F1 (arkosic sand); F1a (grayish brown sandy clay); F2 (black mat); F2b (white marl). From Murray Springs Profile B1, from bottom to top: F1 (arkosic sand); F2a1a: black clay; F1a1: sandy clay; F2b2: white marl from Murray Springs right bank at Curry Draw at North end Trench 22: F2/D, Lower YD Boundary/olive green sandy mudstone.

†Os, Ir, Ru, Pt, and Pd values of the continental crust are from ref. 1; Rh and Au values are from ref. 2.

‡To cover the entire suite of PGEs and Au in the Clearwater East impact melt, the values reported here are those of sample DWC-2-63-1045 analyzed by ref. 3 This is the only PGE enriched impact melt sample of the Clearwater East impact structure that was measured for Pt. To obtain a workable value for the Os concentration, the Os/Ir ratio obtained by ref. 4 was multiplied with the corresponding Ir concentration.

1. Esser BK, Turekian KK (1993) The osmium isotopic composition of the continental crust. *Geochim Cosmochim Acta* 57:3093–3104.
2. Wedepohl KH (1995) The composition of the continental crust. *Geochim Cosmochim Acta* 59:1217–1232.
3. Evans NJ, Gregoire DC, Grieve RAF, Goodfellow WD, Veizer J (1993) Use of platinum-group elements for impactor identification: Terrestrial impact craters and Cretaceous–Tertiary boundary. *Geochim Cosmochim Acta* 57:3737–3748.
4. McDonald I (2002) Clearwater East impact structure: A re-interpretation of the projectile type using new platinum-group element data from meteorites. *Meteoritics Planet Sci* 37:459–464.

Table S2. Comparison of Ir and Pt concentration from International Rock Standard Reference material (TDB-1) between UH, VUB, and WHOI

	Ir, ng/g	Pt, ng/g
TDB-1 UH ($n = 6$)	0.086 ± 0.12	5.4 ± 0.3
TDB-1 VUB ($n = 3$)	0.12 ± 0.004	4.8 ± 1.0
TDB-1 WHOI ($n = 8$)	0.078 ± 0.05	4.4 ± 0.2

Table S3. $^{187}Os/^{188}Os$, Ir, and Pt concentrations from two samples batches, Lake Hind, Manitoba, Canada

Sample	$^{187}Os/^{188}Os$	2 SD	Os, pg/g	Ir, pg/g	Pt, pg/g
FSH 16/18 cm*	ND		ND	38	1,268
FSH 30/32 cm*	1.833	0.018	22	75	918
FSH 30/32 cm REP*	1.933	0.011	104	49	381
FSH 32/34 cm*	2.072	0.021	16	48	921
FH1 23/25 cm†	1.940	0.007	90	69	584
FH1 27/29 cm†	1.864	0.020	114	ND	ND
Fh1 29/31 cm†	1.977	0.008	96	117	474
FH1 31–33 cm†	2.016	0.004	77	25	623
FH1 33–35 cm†	2.039	0.003	77	33	447
FH1 35/37 cm†	1.998	0.005	72	32	457
FH1 37/39 cm†	1.763	0.003	73	43	435
FSH 39/41 cm†	1.738	0.004	73	28	455

ND, not determined.
*Batch 1.
†Batch 2 .

Table S4. $^{187}Os/^{188}Os$, Ir, and Pt concentrations from DSDP 480 (Gulf of California) and ODP 1002C (Cariaco Basin)

Sample	Depth, mbsf	Age, ka	$^{187}Os/^{188}Os$	2 SD	Os, pg/g	Ir, pg/g	Pt, pg/g
480–2H-3W-79/81	8.59	9.32	1.073	0.007	148	ND	ND
480–3H-1W-7/9	9.57	10.55	1.077	0.007	158	23	565
480–3H-1W-23/25	9.73	10.76	1.071	0.014	166	ND	ND
480–3H-1W-54/56	10.04	11.15	1.082	0.007	132	38	ND
480–3H-1W-78/80	10.28	11.45	1.086	0.007	129	ND	ND
480–3H-1W-82/84	10.32	11.50	1.090	0.016	140	17	574
480–3H-1W-89/91	10.39	11.59	0.726	0.028	138	74	ND
480–3H-1W-89/91 REP	10.39	11.59	1.044	0.014	160	54	686
480–3H-1W-98/100	10.48	11.77	1.079	0.003	128	15	595
480–3H-1W-103/105	10.53	11.86	1.078	0.006	138	16	639
480–3H-1W-107/109	10.57	11.93	1.082	0.002	153	16	808
480–3H-1W-112/114	10.62	12.02	1.081	0.004	135	17	717
480–3H-1W-123/125	10.73	12.20	1.081	0.005	138	14	658
480–3H-1W-132/134	10.82	12.36	1.082	0.003	116	14	574
480–3H-1W-141/143	10.91	12.50	1.081	0.006	133	13	706
480–3H-2W-17/19	11.17	12.91	1.082	0.005	122	14	644
480–3H-2W-37/39	11.37	13.03	1.085	0.011	130	10	381
480–3H-2W-51/53	11.51	13.12	1.084	0.006	110	17	517
480–3H-2W-78/80	11.78	13.28	ND		ND	19	627
480–3H-2W-98/100	11.98	13.41	1.086	0.009	117	ND	ND
480–3H-2W-131/133	12.31	13.61	1.090	0.024	106	17	625
480–3H-2W-139/141	12.39	13.66	1.087	0.008	106	67	506
480–3H-3W-17/19	12.67	13.83	1.090	0.008	123	ND	ND
480–3H-3W-33/36	12.83	13.93	1.089	0.012	121	32	618
480–3H-3W-41/44	12.91	13.97	1.092	0.009	110	ND	ND
1002C-1H-3W-40.0/42.0	3.4	9.19	1.036	0.005	111	26	553
1002C-1H-3W-46.0/48.0	3.46	9.34	1.034	0.004	185	44	939
1002C-1H-3W-59.0–61.0	3.59	9.67	1.022	0.005	172	49	1151
1002C-1H-3W-70.0/72.0	3.7	9.95	1.035	0.006	167	44	746
1002C-1H-3W-80.0/82.0	3.8	10.20	1.026	0.003	171	39	868
1002C-1H-3W-89.0/91.0	3.89	10.43	1.005	0.004	150	43	753
1002C-1H-3W-99.0/100.0	3.99	10.69	1.035	0.009	169	32	1222
1002C-1H-3W-110.0/112.0	4.1	10.97	1.032	0.009	128	31	588
1002C-1H-3W-120.0/122.0	4.2	11.22	1.011	0.006	133	51	862
1002C-1H-3W-130/132	4.3	11.47	1.020	0.004	127	27	727
1002C-1H-3W-132.0/134.0	*4.3*	*11.47*	*1.045*		*165*		
1002C-1H-4W-8.0/10.0	4.58	12.30	1.047	0.010	105	ND	ND
1002C-1H-4W-15.0/17.0	4.65	12.50	1.034	0.003	196	49	861
1002C-1H-4W-27.5/29.5	4.775	12.80	1.025	0.004	97	22	705
1002C-1H-4W-35.0/37.0	4.85	13.01	1.044	0.005	124	30	633
1002C-1H-4W-55.0/57.0	5.05	13.59	1.048	0.006	100	41	963
1002C-1H-4W-64.0/66.0	5.14	13.78	1.039	0.004	105	33	982
1002C-1H-4W-75.0/77.0	5.25	14.06	1.031	0.003	121	30	832

The sample in italic type is from ref. 1. mbsf, meters below sea floor; ND, not determined.

1. Oxburgh R, Pierson-Wickma A-C, Reisberg L, Hemming S (2007) Climate-correlated variations in seawater $^{187}Os/^{188}Os$ over the past 200,000 yr: Evidence from the Cariaco Basin, Venezuela. *Earth Planet Sci Lett* 263:246–258.